[14] D. A. Huse, S. Leibler, *J. Phys.* **1988**, *49*, 605.
[15] J. Allgaier, A. Poppe, L. Willner, D. Richter, *Macromolecules* **1997**, *30*, 1582.
[16] A. C. Finnefrock, G. E. S. Toombes, S. M. Gruner, R. Ulrich, U. Wiesner, unpublished results.
[17] S. Brunauer, L. S. Deming, W. S. Deming, E. Teller, *J. Am. Chem. Soc.* **1940**, *62*, 1723.
[18] E. P. Barrett, L. G. Joyner, P. P. Halenda, *J. Am. Chem. Soc.* **1951**, *73*, 373.
[19] S. J. Gregg, K. S. W. Sing, *Adsorption, Surface and Porosity*, 2nd ed., Academic Press, **1982**.
[20] J. M. Thomas, *Angew. Chem.* **1999**, *111*, 3800–3843; *Angew. Chem. Int. Ed.* **1999**, *38*, 3588–3628.
[21] P. Ström, D. M. Anderson, *Langmuir* **1992**, *8*, 691.
[22] M. W. Tate, S. M. Gruner, E. F. Eikenberry, *Rev. Sci. Instrum.* **1997**, *68*, 47.

Solvent-Free, Low-Temperature, Selective Hydrogenation of Polyenes using a Bimetallic Nanoparticle Ru–Sn Catalyst**

Sophie Hermans, Robert Raja, John M. Thomas,* Brian F. G. Johnson,* Gopinathan Sankar, and David Gleeson

Progress in making solvent-free chemical conversions much more feasible than they are at present awaits the development of highly active (and selective) heterogeneous catalysts. Not only must the sites at which turnover occurs be of high intrinsic activity, their concentration (per unit mass) must also be large. Moreover, diffusion of reactant species to, and of products away from, such sites must also be facile.[1]

Herein we demonstrate how freely accessible active sites on bimetallic nanoparticles, finely dispersed and firmly anchored along the interior surfaces of high area (around 800 $m^2 g^{-1}$) mesoporous silica function as highly effective catalysts for a number of selective hydrogenations that are of considerable significance for chemical and fine-chemical production. Such heterogeneous nanocatalysts may be readily prepared[2–5] from mixed-metal carbonylates and introduced in a spatially uniform fashion along the pores (around 30 Å diameter) of the silica host. Their atomic structure is straightforwardly established,[1, 6–8] from in situ X-ray absorption and FTIR measurements.

Tin has been widely used as a "promoter" in heterogeneous catalysis, and has been shown to increase dramatically the selectivity of ruthenium catalysts in a variety of chemical transformations. These usually involve the selective hydrogenation of a carbonyl group in the vicinity of a conjugated or isolated double bond, such as the hydrogenation of benzoic acid and fatty esters to their corresponding alcohols[9, 10] or the hydrogenation of acrolein and its derivatives.[11] It has been suggested that the effect of tin is, besides others, to deactivate selectively certain catalytic sites on the surface thereby impeding undesirable side reactions.[10, 12] Other explanations, such as alloying and its consequential electronic influences, have also been proposed.[11]

The chemical conversions upon which we focus herein consist of the hydrogenation of cyclic polyenes: 1,5,9-cyclododecatriene, 1,5-cyclooctadiene, and 2,5-norbornadiene. The monoenes of all three polyenes are used extensively as intermediates in the synthesis of bicarboxylic aliphatic acids, ketones, cyclic alcohols, lactones, and other intermediates. The selective hydrogenation of 1,5,9-cyclododecatriene to cyclododecane and cyclododecene is industrially important in the synthesis of valuable organic and polymer intermediates, such as 12-laurolactam and dodecanedioic acid,[13] which are important monomers for nylon 12, nylon 612, copolyamides, polyesters, and coating applications.

A wide variety of homogeneous and heterogeneous hydrogenation catalysts such as Raney nickel,[14] palladium,[15] platinum,[16] cobalt,[17] and mixed transition-metal complexes have been previously used for the above-mentioned hydrogenations.[18, 19] But all the reactions entailed the use of organic solvents (such as *n*-heptane, benzonitrile, and so forth),[13, 20–22] and some required utilization of efficient hydrogen donors such as 9,10-dihydroanthracene, often at temperatures in excess of 300 °C, to achieve the desired selectivities.[23] Recently, Reetz et al.[24] have shown that entrapment of palladium clusters in micro/mesoporous hydrophobic sol–gel matrices prevents undesired agglomeration of the clusters, to result in active catalysts for the hydrogenation of 1,5-cyclooctadiene.

Previously, we have described the catalytic performance of other, finely dispersed bimetallic catalysts (Ag–Ru,[2] Cu–Ru,[3] and Pd–Ru,[4]), some of which possessed remarkable properties. Herein we report the catalytic performance of a supported carbidic Ru_6Sn nanoparticle and compare it with that of the above-mentioned bimetallic nanocatalysts. In particular, we highlight the changing selectivity (in the hydrogenation of 1,5,9-cyclododecatriene and other polyenes) as a function of operating temperature and degree of conversion.

The compound (PPN)$[Ru_6C(CO)_{16}SnCl_3]$ (PPN: bis(triphenylphosphane)iminium cation) is obtained in a two step reaction from the known carbido–hexaruthenium cluster $[Ru_6C(CO)_{17}]$. Details of the preparation along with the single-crystal X-ray structure of the anion $[Ru_6C(CO)_{16}SnCl_3]^-$ (**1**), have been given elsewhere,[25] as have the corresponding details for the neutral species

[*] Prof. Sir J. M. Thomas, Dr. G. Sankar, Dr. D. Gleeson
The Royal Institution of Great Britain
Davy Faraday Research Laboratory
21 Albemarle Street, London W1X 4BS (UK)
Fax: (+44) 0207-670-2988
E-mail: dawn@ri.ac.uk

Prof. B. F. G. Johnson, S. Hermans, Dr. R. Raja
Department of Chemistry
University of Cambridge
Lensfield Road, Cambridge CB2 1EW (UK)
Fax: (+44) 1223-339016
E-mail: jpt25@cam.ac.uk

[**] We thank Dr. R. G. Bell for assistance with the computer graphics, Drs. P. A. Midgeley, V. Keast, and M. Weyland for help with STEM, and gratefully acknowledge the support (via a rolling grant to J.M.T. and an award to B.F.G.J.) of EPSRC and the award of a research fellowship (for G.S.) from the Leverhulme Foundation and a Marie Curie Fellowship within the TMR Programme of the European Commission (for S.H.).

  0044-8249/01/11307-1251 $ 17.50+.50/0

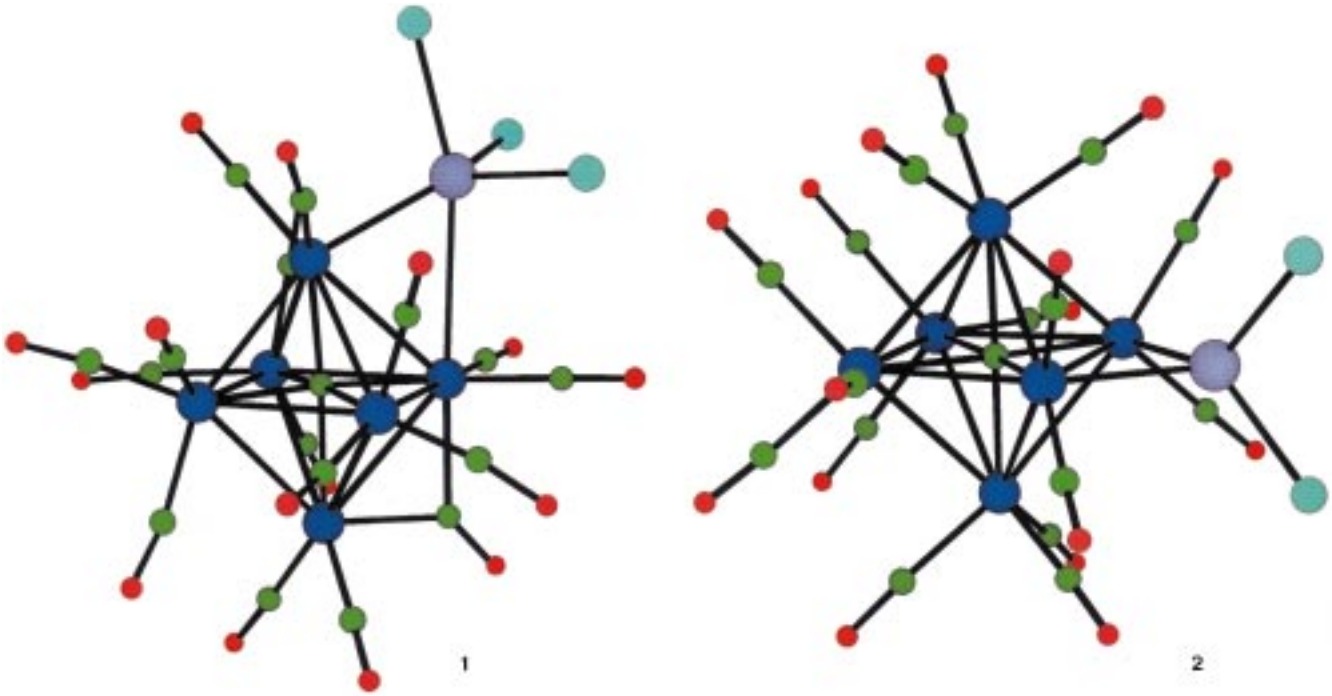

Figure 1. Molecular structures of $[Ru_6C(CO)_{16}SnCl_3]^-$ **1** and $[Ru_6C(CO)_{16}SnCl_2]$ **2**, as determined by X-ray crystallography.

$[Ru_6C(CO)_{16}SnCl_2]$ (**2**; see Figure 1). This latter compound can be obtained by chloride abstraction from **1** or directly by reacting $[Ru_6C(CO)_{17}]$ with $SnCl_2$. The mesoporous silica was loaded with cluster **1** by making a slurry in ether/dichloromethane, stirring for 48 h under nitrogen, and filtering.[3] The pink solid obtained was then washed with ether and dried under vacuum. The same procedure was used for the incorporation of cluster **2** within the mesopores. However, a small amount of nonadsorbed compound was lost in the filtrate, demonstrating the less favorable interaction of this neutral species with the surface hydroxyl groups of MCM-41, when compared to its charged analog **1**.

The catalytic precursor material **1**/MCM-41, which was characterized by FTIR (using a purpose-built evacuable cell[7]), revealed that the carbonyl cluster was still intact within the pores. This was confirmed by extended x-ray absorption fine structure (EXAFS) analysis, which showed that the structure of the pure, unsupported carbonyl cluster is exactly identical to that of the species adsorbed into the mesoporous silica.

The frequency characteristics of the terminal carbonyl groups disappeared totally at a heat-treatment temperature of 200 °C. During this activation procedure—and concomitant with the loss of all carbonyl ligands—the metallic core of the cluster becomes firmly anchored to the siliceous surface (Figure 2).

The EXAFS data, recorded in situ,[2, 3] showed significant changes in the coordination environment of both the tin and ruthenium centers (Figure 3). The best fit for the ruthenium K-EXAFS data yielded a structure for the denuded bimetallic catalyst consisting of mainly ruthenium neighbours. To obtain a better fit for the low k data, it was necessary to include a carbon neighbour. The Ru–Ru and Ru–C distances and the coordination number of 2.67 and 2.07 Å, and 3 and 1, respectively, suggest that the arrangement of Ru, C, and Sn are quite similar to that of the starting material. Upon removal of the carbonyl ligands the Ru–Ru distances decreased from an average value of around 2.8 to 2.67 Å. It is not directly feasible to detect the Ru–Sn interaction, since only one of the six ruthenium centers has a close contact with the tin atom. Similarly, from the Sn K-edge, two of the chlorine neighbors are completely replaced by the oxygen atoms, and the best fit is obtained by taking two Sn–O, one Sn–Cl, and one Sn–Ru interaction,[26] which shows that the tin atom is the anchoring point of the bimetallic, nanoparticle

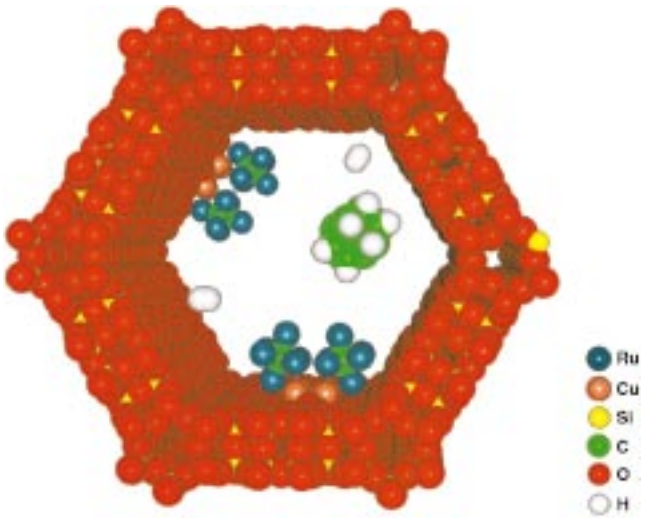

Figure 2. Computer graphic model of $Cu_4Ru_{12}C_2$ nanocatalyst clusters anchored through pendant silanol groups to the inner walls of mesoporous silica (MCM-41). This nanocatalyst is akin to Ru_6Sn and other clusters described in the text. A typical reactant (1,5,9-cyclododecatriene) and H_2 are also shown in the mesopore channel (diameter around 30 Å).

  0044-8249/01/11307-1252 $ 17.50+.50/0

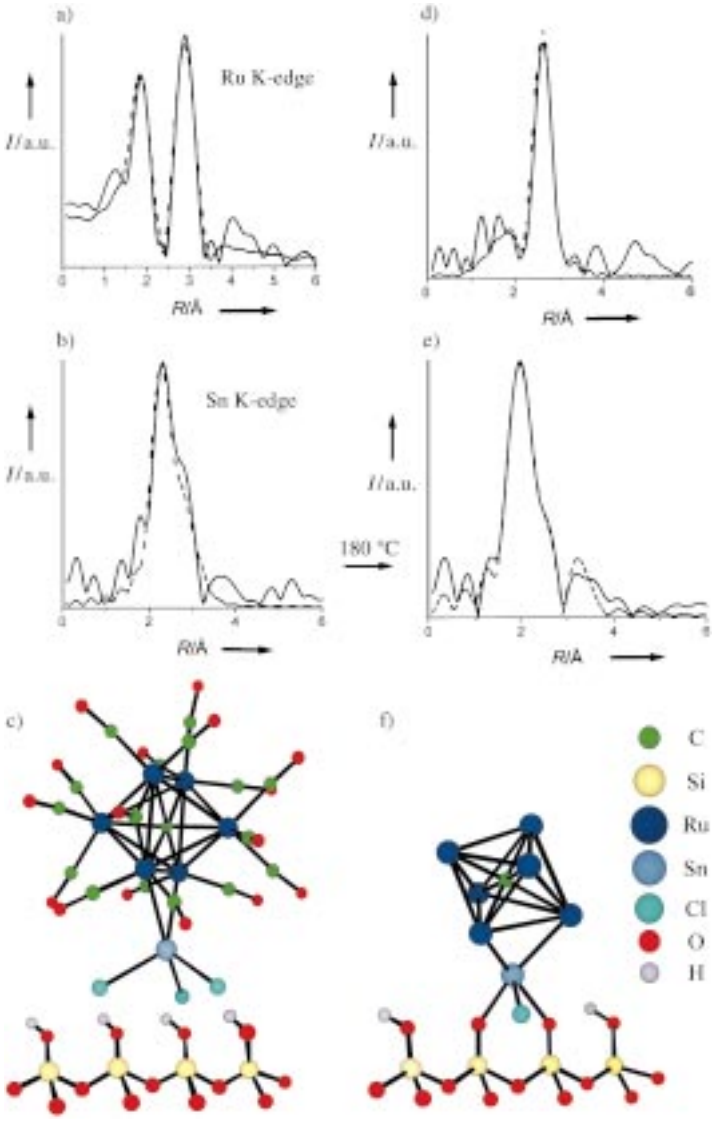

Figure 3. Fourier transform of the EXAFS a) at the Ru K-edge and b) Sn K-edge (of the $[Ru_6C(CO)_{16}SnCl_3]^-$ cluster anchored on MCM-41. c) The single crystal-derived structure is broadly consistent with the experimental EXAFS data. Fourier transforms of the d) Ru K-edge and e) Sn K-edge EXAFS of the decarbonylated (by mild thermolysis at 180 °C in vacuum for 1 h) catalysts. f) Local structure of the activated catalyst, derived from the analysis of the EXAFS data. Solid and dashed lines in (a), (b), (d) and (e) represent the experimental and calculated data, respectively.

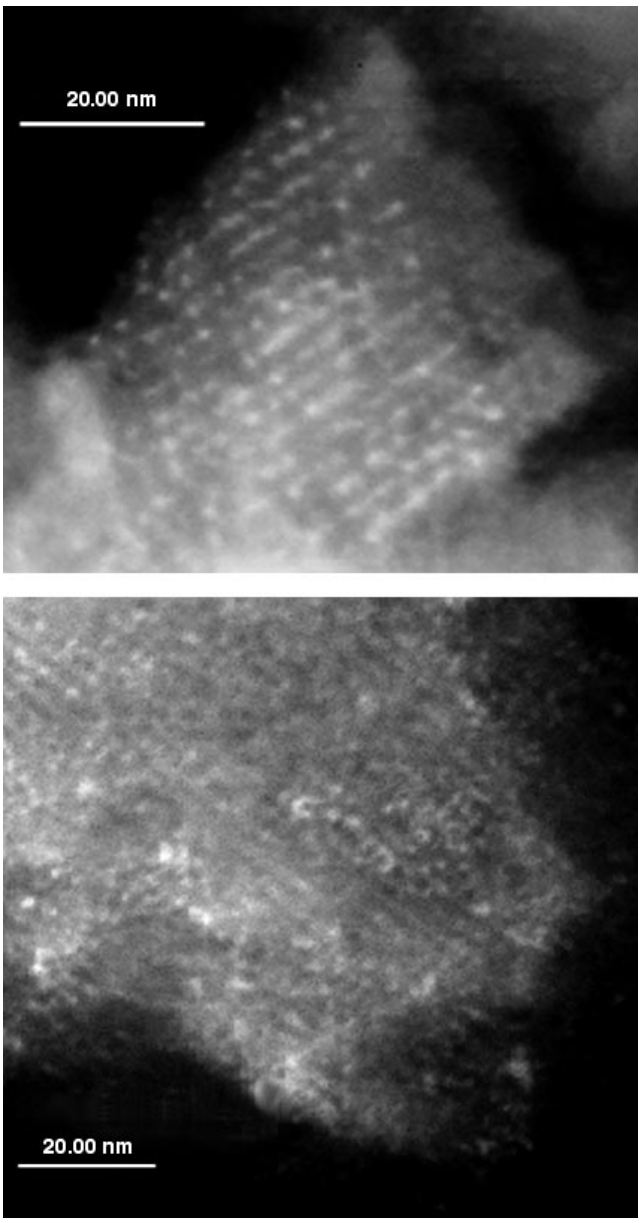

Figure 4. High-angle, annular dark field electron micrographs of the Ru_6Sn/MCM-41 catalyst a) prior to and b) after catalytic use.

catalyst on the silica surface. Taking these results into account, we propose a model for the active denuded cluster that is shown in Figure 3 f. We found that cluster **2** could not be freed completely from its residual chlorine ligands; in fact, the Ru K-edge EXAFS data could be refined only on the assumption that a residual chlorine atom was attached to the ruthenium centers. Furthermore, this denuded material derived from cluster **2** is not catalytically active.[27]

High-angle, annular dark-field (HAADF) scanning transmission electron microscopy (STEM),[1, 5] shows (Figure 4) how well the nanoparticle catalysts are distributed within the mesopores of the silica support both prior to and after catalytic testing (see below). No dramatic change in the structure of the material (such as sintering of the nanoparticles or breakdown of the MCM-41 matrix) occurs during catalysis. This demonstrates both the robust nature of the nanoparticle catalyst and its effective anchoring to the walls of the high-area silica. The overall composition and the invariance of the ratio of the two metals were deduced from energy-dispersive X-ray analysis on both the as-prepared and used specimens of catalyst. Consistent with the fact that no Sn – Sn bond were detected by EXAFS, this indicates that each nanoparticle is derived from an intact cluster core made of six ruthenium atoms, one carbon atom and a single atom of tin.

The marked dependence of temperature upon selectivity in the catalytic hydrogenation of 1,5,9-cyclododecatriene is shown in Figure 5 , from which we note that, even as low as 80 °C, this solvent-free hydrogenation to cyclododecene is 70 % selective and well in excess of 90 % at 100 °C. This

  0044-8249/01/11307-1253 $ 17.50+.50/0

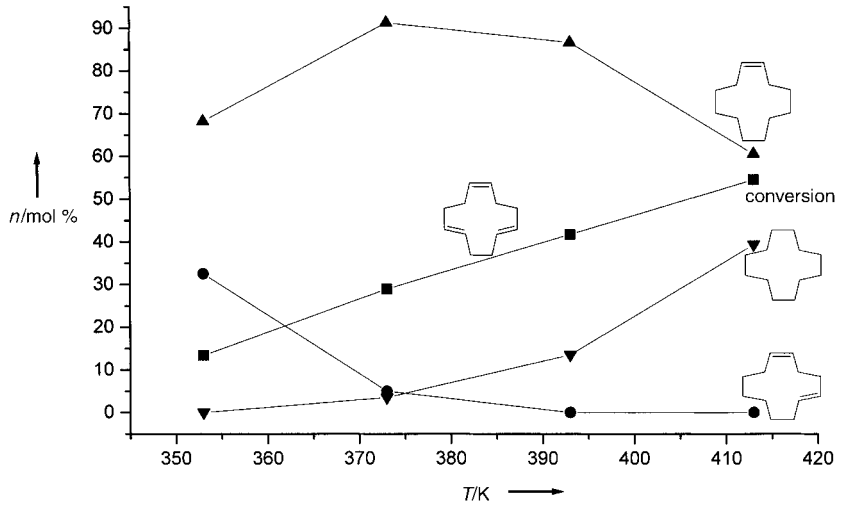

Figure 5. The effect of temperature on the hydrogenation conversion (■) of the prodcut selectivity is marked in terms of singly (●), doubly (▲), and fully (▼) hydrogenated products of 1,5,9-cyclododecatriene with the Ru_6Sn catalyst.

particular selective hydrogenation falls off in efficiency with further increase in temperature, and conversion to the fully hydrogenated cyclododecane is progressively favored. It is noteworthy that conversion to the cyclododecadiene on the other hand is favored at the lowest test temperature (80 °C). By contrast, the Pd_6Ru_6 catalyst reported earlier[4] displays very little selectivity for the 1,5-cyclododecadiene or cyclododecene, even at temperatures as low as 40 °C. By comparison with three other bimetallic catalysts (Cu_4Ru_{12}, Ag_4Ru_{12} and Pd_6Ru_6), we note that precursor **1** yields the bimetallic catalyst (Ru_6Sn) with the best performance, so far as selective hydrogenation of one of the two double bonds in the hydrogenation of 1,5-cyclooctadiene is concerned (Figure 6).

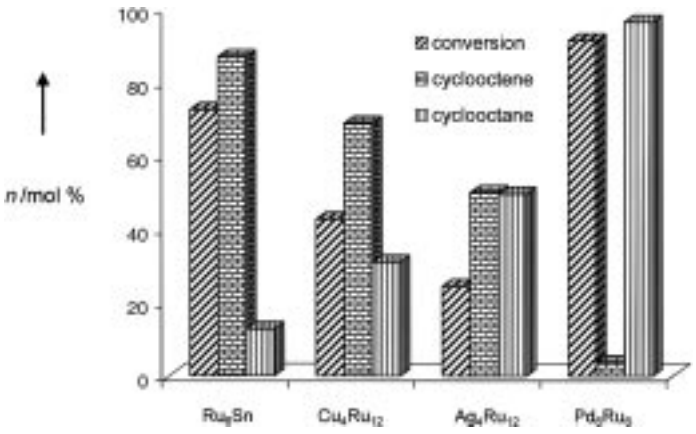

Figure 6. Comparison of catalytic performance and degree of selectivity for the hydrogenation of 1,5-cyclooctadiene, after 24 h, at 353 K. (See Table 1 for reaction conditions).

Further scope for fine-tuning both the conversion and selectivity is obtained by varying the contact times, for a range of polyenes (Table 1). It is particularly interesting that, in the case of 2,5-norbornadiene, the conditions (and catalyst) may be so chosen as to produce a high yield of either norbornene or norbornane. It is also evident from Table 1 that bimetallic nanoparticle catalysts are far superior in performance to their monometallic analogs and more importantly yield a higher selectivity for hydrogenated products, which shows a synergism between the two components of the bimetallic nanoparticle. We established in separate experiments that monometallic Ru_6 and Pd anchored on MCM-41 were inactive for the above-mentioned reactions. Considerable scope clearly exists, with the principles that we have outlined here and previously to develop other, solvent-free systems for the selective conversion of organic compounds.

We have demonstrated how to regulate the selectivity of nanocatalysts for solvent-free hydrogenations by changing the nature of the constituents in its active phase.

Experimental Section

Electron Microscopy: The images were obtained on a VG HB501 field-emission STEM microscope. A small amount of activated catalyst was ground and suspended in hexane by ultrasonic treatment. A holey carbon film supported on a copper grid was dipped into the solution and allowed to dry in the air before introduction to the microscope. The sample dispersed on the grid was further dried inside the preparation chamber of the microscope by heating at ca. 100 °C under a light bulb and then was left under high vacuum overnight before acquiring the images.

EXAFS: Ru and Sn K-edge EXAFS data were collected at station 9.2 at the Daresbury Synchrotron Laboratory, which operates at 2 GeV and a typical current in the range of 150 to 250 mA. This station is equipped with a quick scanning Si(220) double-crystal monochromator, ion chambers for measuring incident (I_0), transmitted (I_t) beam intensities, and a 13 element Canberra fluorescence detector. In a typical experiment 150 mg of the sample was pressed into a self-supporting wafer and loaded in to the in situ cell.[28] The cell was evacuated to around 4×10^{-3} Torr and the catalyst was heated to 180 °C at 5 K min^{-1} and retained at this temperature for around 1 h before cooling it to room temperature. All the EXAFS experiments were performed in the fluorescence mode and 10 scans were taken to improve the signal to noise ratio. The data processing was done using the suite of programs available at Daresbury, namely, EXCALIB, EXBROOK, and EXCURV98. The summed data were analysed without Fourier filtering and a full multiple scattering procedure was employed to analyse all the data sets, in particular when carbonyl species and second silicon neighbors were included in the analysis.

Catalysis: The catalytic testing was carried out in a high-pressure stainless steel reactor (Cambridge Reactor Design) lined with PEEK (polyetheretherketone). Nanoparticle bimetallic catalyst (20 mg) was activated (473 K, 2 h, in the presence of hydrogen (0.5 MPa) prior to the hydrogenation reaction. The reactor was then depressurised and cooled to room temperature, before introducing the substrate (50 g;see Table 1) and internal standard (mesitylene, 2.5 g). The vessel was pressurised with hydrogen (30 bar) and heated to the desired temperature with continued stirring (400 min^{-1}). During the reaction, small aliquots were removed, using a mini-robot autosampler, to enable the kinetics to be studied. The products of the reaction were analysed with gas chromatograpy (GC, Varian, Model 3400 CX) employing a HP-1 capillary column (25 m × 0.32 mm) and flame ionisation detector. The identity of the products was confirmed by LC-MS (Shimadzu, QP 8000).

Both the Ru_6Sn and Pd_6Ru_6 bimetallic nanoparticle anchored catalysts were reused six or seven times for the hydrogenation of 1,5-cyclooctadiene and 1,5,9-cyclododecatriene without appreciable loss in catalytic activity or

  0044-8249/01/11307-1254 $ 17.50+.50/0

Table 1. Hydrogenation of polyenes—comparison of catalysts.

Catalyst	Substrate	t [h]	T [K]	Conv. [mol %]	TOF[a] [h^{-1}]	Prod. dist. [mol %]		
						A	B	
Ru_6Sn/MCM-41	1,5-cyclooctadiene	8	353	11.7	1980	100	–	
		24		72.5	4090	86.9	12.8	
Cu_4Ru_{12}/MCM-41	1,5-cyclooctadiene	8	353	11.5	690	70.4	29.2	
		24		42.7	1422	68.8	31.0	
Ag_4Ru_{12}/MCM-41	1,5-cyclooctadiene	8	353	9.0	465	57.3	42.5	
		24		24.4	1316	50	49.6	
Pd_6Ru_6/MCM-41	1,5-cyclooctadiene	8	353	36.9	2012	15.7	84.5	
		24		91.4	4965	3.6	96.5	
Ru_6/MCM-41	1,5-cyclooctadiene	24	353	2.5	141	–	36.2	
Pd/MCM-41	1,5-cyclooctadiene	24	353	7.3	212	–	100	
						C	D	E
Ru_6Sn/MCM-41	1,5,9-cyclododecatriene	8	353	4.7	530	84.0	15.8	–
		24		13.4	503	32.5	68.2	–
Ru_6Sn/MCM-41	1,5,9-cyclododecatriene	8	373	17.2	1940	17.2	82.4	–
		24		28.9	1130	5.0	91.3	3.5
Ru_6Sn/MCM-41	1,5,9-cyclododecatriene	8	393	28.2	3280	6.8	87.0	6.0
		24		41.7	1785	–	86.7	13.5
Ru_6Sn/MCM-41	1,5,9-cyclododecatriene	8	413	39.1	4400	–	80.2	19.5
		24	–	54.5	2170	–	60.5	39.3
Pd_6Ru_6/MCM-41	1,5,9-cyclododecatriene	8	353	47.2	3320	–	48.2	51.5
		24		62.0	1975	–	36.2	63.6
Pd_6Ru_6/MCM-41	1,5,9-cyclododecatriene	8	373	64.9	5350	–	11.7	88.5
		24		86.2	3200	–	6.2	95.7
						F	G	
Ru_6Sn/MCM-41	2,5-norbornadiene	8	333	51.4	10210	88.6	11.3	
		24		89.3	5960	46.8	53.3	
Pd_6Ru_6/MCM-41	2,5-norbornadiene	8	333	76.4	11176	24.7	75.1	
		24		98.7	6855	2.5	97.6	

[a] TOF = $[(mol_{substr})(mol_{cluster})^{-1}h^{-1}]$. Reaction conditions: substrate ≈ 50 g; catalyst = 25 mg; H_2 pressure = 30 bar; A = cyclooctene; B = cyclooctane; C = 1,9-cyclododecadiene; D = cyclododecene; E = cyclododecane; F = norbornene; G = norbornane; .

selectivity. In addition, the following experiments were performed to rule out the possibility of leaching:

- In a typical experiment (see Table 1 and Figure 6), the solid catalyst was filtered from the reaction mixture (when hot) after 8 h, and the reaction was continued with the resulting filtrate for a further 16 h. No significant change in conversion or product selectivity was observed, indicating that the metal ions leached out (if any) are not responsible for the observed activity and selectivity.
- The resulting filtrate (at the end of the reaction, after 24 h) was independently analyzed by ICP and AAS for free or dissolved metal (Sn, Pd, Ru) ions, and only trace amounts (<3 ppb) were detected.

Received: November 20, 2000 [Z16135]

[1] J. M. Thomas, *Angew. Chem*. **1999**, *111*, 3800; *Angew. Chem. Int. Ed.* **1999**, *38*, 3589.
[2] D. S. Shephard, T. Maschmeyer, B. F. G. Johnson, J. M. Thomas, G. Sankar, D. Ozkaya, W. Z. Zhou, R. D. Oldroyd, R. G. Bell, *Angew. Chem*. **1997**, *109*, 2337; *Angew. Chem. Int. Ed. Engl*. **1997**, *36*, 2242.
[3] D. S. Shephard, T. Maschmeyer, G. Sankar, J. M. Thomas, D. Ozkaya, B. F. G. Johnson, R. Raja, R. D. Oldroyd, R. G. Bell, *Chem. Eur. J.* **1998**, *4*, 1214.
[4] R. Raja, S. Hermans, D. S. Shephard, S. Bromley, J. M. Thomas, B. F. G. Johnson, T. Maschmeyer, *Chem. Commun*. **1999**, 2131.
[5] D. Ozkaya, W. Z. Zhou, J. M. Thomas, P. Midgeley, V. J. Keast, S. Hermans, *Catal. Lett*. **1999**, *60*, 113.
[6] J. M. Thomas, *Chem. Eur. J.* **1997**, *3*, 1557.
[7] G. Sankar, J. M. Thomas, *Top. Catal*. **1999**, *8*, 1.
[8] J. M. Thomas, G. Sankar, *J. Synchrotron Radiat*. **2000**, in press.
[9] K. Ishii, F. Mizukami, S. Niwa, R. Kutsuzawa, M. Toba, F. Fujii, *Catal. Lett*. **1998**, *52*, 49.
[10] V. M. Deshpande, K. Ramnarayan, C. S. Narasimhan, *J. Catal*. **1990**, *121*, 174.
[11] B. Coq, F. Figueras, C. Moreau, P. Moreau, M. Warawdekar, *Catal. Lett*. **1993**, *22*, 189.
[12] G. Neri, R. Pietropaolo, S. Galvagno, C. Milone, J. Schwank, *J. Chem. Soc. Faraday Trans.* **1994**, *90*, 2803.
[13] J. Hanika, I. Svoboda, V. Ruzicka, *Coll. Czech. Chem. Commun.* **1981**, *46*, 1039.
[14] Y. Kurokawa, UPE Industries Ltd, Jap. Patent 6,274,938, **1987**.
[15] G. Strukul, G. Carturan, *Inorg. Chim. Acta* **1979**, *35*, 99.
[16] C. A. Brown, H. C. Brown, *J. Org. Chem*. **1966**, *31*, 3989.
[17] R. E. Harmon, S. K. Gupta, D. J. Brown, *Chem. Rev.* **1973**, *73*, 21.
[18] BASF, Ger. Patent 1,230,790.
[19] BASF, UK Patent 826,832.
[20] C. Ruchardt, M. Gerst, M. Nolke, *Angew. Chem*. **1992**, *104*, 1516; *Angew. Chem. Int. Ed. Engl.* **1992**, *31*, 1523.
[21] C. Hofler, C. Ruchardt, *Liebigs Ann*. **1995**, 183.
[22] M. Gerst, C. Ruchardt, *Tetrahedron Lett*. **1993**, *34*, 7733.
[23] J. Morgenthaler, C. Ruchardt, *Liebigs Ann*. **1996**, 1529.
[24] M. T. Reetz, M. Dugal, *Catal. Lett*. **1999**, *58*, 207.
[25] S. Hermans, B. F. G. Johnson, *Chem. Commun*. **2000**, 1955.
[26] We endeavoured, but failed, to detect this chlorine atom(present in trace amounts) by electron-stimulated X-ray emission, using an energy-dispersive analyzer inside our scanning electron microscope, due to overlap with strong peaks corresponding to ruthenium.
[27] A more detailed structure analysis of this material, which is not discussed further here, will be published elsewhere.
[28] P. A. Barrett, G. Sankar, C. R. A. Catlow, J. M. Thomas, *J. Phys. Chem. A* **1996**, *100*, 8977.